

## Cole cole time fractal dimension for characterizing Shajara Reservoirs of the Permo-Carboniferous Shajara Formation, Saudi Arabia

Khalid Elyas Mohamed Elameen Alkhidir <sup>1\*</sup>

Department of Petroleum and Natural Gas Engineering, College of Engineering King Saud University, Saudi Arabia

**\*Corresponding author:** Prof. Khalid Elyas Mohamed Elameen Alkhidir Ph.D, Department of Petroleum and Natural Gas Engineering, College of Engineering King Saud University, Saudi Arabia; Email: kalkhidir@ksu.edu.sa

**Citation:** Khalid Elyas Mohamed Elameen Alkhidir (2019) Cole cole time fractal dimension for characterizing Shajara Reservoirs of the Permo-Carboniferous Shajara Formation, Saudi Arabia: Nessa J of Environmental Sciences.

**Received:** 4<sup>th</sup> April 2019; **Accepted:** 9<sup>th</sup> May 2019; **Published:** 7<sup>th</sup> June 2019

**Copyright:** © 2019 Khalid Elyas Mohamed Elameen Alkhidir. This is an open-access article distributed under the terms of the Creative Commons Attribution License, which permits unrestricted use, distribution, and reproduction in any medium, provided the original author and source are credited.

### Abstract

The quality and assessment of a reservoir can be documented in details by the application of cole cole time. This research aims to calculate fractal dimension from the relationship among cole cole time, maximum cole cole time and water saturation and to confirm it by the fractal dimension derived from the relationship among capillary pressure and water saturation. In this research, porosity was measured on real collected sandstone samples and permeability was calculated theoretically from capillary pressure profile measured by mercury intrusion techniques. Two equations for calculating the fractal dimensions have been employed. The first one describes the functional relationship between wetting phase saturation, cole cole time, and maximum cole cole time and fractal dimension. The second equation implies to the wetting phase saturation as a function of capillary pressure and the fractal dimension. Two procedures for obtaining the fractal dimension have been utilized. The first procedure was done by plotting the logarithm of the ratio between cole cole time and maximum cole cole time versus logarithm wetting phase saturation. The slope of the first procedure is positive =  $3 - D_f$  (fractal dimension). The second procedure for obtaining the fractal dimension was completed by plotting logarithm of capillary pressure versus the logarithm of wetting phase saturation. The slope of the second procedure is negative =  $D_f - 3$ . On the basis of the obtained results of the fabricated stratigraphic column and the attained values of the fractal dimension, the sandstones of the Shajara reservoirs of the Shajara Formation were divided here into three units. These units from bottom to top are: Lower Shajara Cole Cole Time Fractal Dimension Unit, Middle Shajara Cole Cole Time Fractal Dimension Unit, and Upper Shajara Cole Cole Time Fractal Dimension Unit. The three reservoir units were also confirmed by capillary pressure fractal dimension. It was found that the obtained fractal dimension increases with increasing grain size and permeability.

**Keywords:** Shajara Reservoirs, Shajara Formation, cole cole time fractal dimension, capillary pressure fractal dimension.

## Introduction

Toledo et al reported that the wetting phase saturation can be described as function of capillary pressure and fractal dimension. Li and Horne. Demonstrated that the Purcell model was found to be the best fit to the experimental data of the wetting phase relative permeability for the cases as long as the measured capillary pressure curve had the same residual saturation as the relative permeability curve. They also reported that in the reverse procedure, capillary pressure could also be computed once relative permeability data are available. Li and Willams Derived theoretically a model to correlate capillary pressure and resistivity index based on the fractal scaling theory. Their results demonstrated that the model could match the experimental data in a specific range of low water saturation. Zhang and Weller showed the fractal dimension resulting from longer transverse NMR relaxation times and lower capillary pressure reflects the volume dimension of larger pores. They also reported that the fractal dimension derived from the short NMR relaxation times is similar to the fractal dimension of the internal surface. Wang et al Reported that the fractal dimensions can be used to represent the complexity degree and heterogeneity of pore structure, and the coexistence of dissolution pores and large intergranular pores of Donghetang sandstones contributes to a heterogeneous pore throat distribution and a high value of fractal dimension. Guo et al studied the relationship among capillary pressure (PC), nuclear magnetic transverse relaxation time (T2) and resistivity index (I). An increase of bubble pressure fractal dimension and pressure head fractal dimension and decreasing pore size distribution index and fitting parameters  $m^*n$  due to possibility of having interconnected channels was confirmed by Alkhidir. An increase of fractal dimension with increasing arithmetic, geometric relaxation time of induced polarization, permeability and grain size was investigated by Alkhidir. An increase of seismo electric and resistivity fractal dimensions with increasing permeability and grain size was described by Alkhidir. An increase of electro kinetic fractal dimension with increasing permeability and grain size was reported by Alkhidir. A transverse relaxation time of nuclear magnetic resonance fractal dimension was reported by Alkhidir.

## Material and Method

Samples were collected from the surface type section of the Shajara reservoirs of the Permo-carboniferous Shajara formation at latitude  $26^{\circ} 52' 17.4''$ , longitude  $43^{\circ} 36' 18''$ . Porosity was measured and permeability was derived from the measured capillary pressure data.

The Cole cole time (Tcc) can be scaled as

$$S_w = \left[ \frac{\sqrt{T_{cc}}}{\sqrt{T_{ccmax}}} \right]^{3-D_f} = \left[ \frac{T_{cc}^{\frac{1}{2}}}{T_{ccmax}^{\frac{1}{2}}} \right]^{3-D_f} \quad 1$$

Where  $s_w$  is the water saturation; Tcc cole cole time in second; Tcc max is the maximum cole cole time in second;  $D_f$  is the fractal dimension

Equation 1 can be proofed from

$$T_{cc} = \frac{A^2}{2D_i} \quad 2$$

Where  $t_{cc}$  is cole cole time in second;  $A$  is the pore throat radius in meter;  $D_i$  is the diffusion coefficient in square meter per second  $m^2/s$ .

The pore throat radius  $A$  can be scales as

$$A = \left[ \frac{[2 * \sigma * \cos\theta]}{pc} \right] \quad 3$$

Where  $\sigma$  is the surface tension;  $\theta$  is the contact angle; and  $pc$  is the capillary pressure.

$$A^2 = \left[ \frac{[4 * \sigma^2 * \cos^2\theta]}{pc^2} \right] \quad 4$$

Insert equation 4 into equation 2

$$T_{cc} = \left[ \frac{[4 * \sigma^2 * \cos^2\theta]}{2 * D_i * pc^2} \right] \quad 5$$

Take the square root of Equation 5

$$\sqrt{T_{cc}} = \sqrt{\left[ \frac{[4 * \sigma^2 * \cos^2\theta]}{2 * D_i * pc^2} \right]} \quad 6$$

$$\sqrt{T_{cc}} = \left[ \frac{[\sqrt{2} * \sigma * \cos\theta]}{[pc * \sqrt{D_i}]} \right] \quad 7$$

The cumulative pore volume can be scaled as

$$v \propto r^{3-D_f} \quad 8$$

$$v \propto pc^{(D_f-3)} \quad 9$$

Differentiate Equation 9 with respect to capillary pressure

$$\frac{\Delta v}{\Delta pc} \propto pc^{D_f-4} \quad 10$$

If we remove the sign of proportionality of equation 10 we have to multiply by a constant.

$$\frac{\Delta v}{\Delta pc} = \text{constant} * pc^{D_f-4} \quad 11$$

Integrate equation 11

$$\int \Delta v = \text{constant} \int_{p_{c\min}}^{p_c} p_c^{Df-4} \Delta P_c \quad 12$$

The result of integral of equation 12

$$v = \frac{\text{constant}}{Df-3} * [p_c^{Df-3} - p_{c\min}^{Df-3}] \quad 13$$

The total pore volume can be integrated as

$$\int \Delta v_{\text{total}} = \text{constant} \int_{p_{c\min}}^{p_{c\max}} p_c^{Df-4} \Delta P_c \quad 14$$

The result of integration of equation 14

$$v_{\text{total}} = \frac{\text{constant}}{Df-3} * [p_{c\max}^{Df-3} - p_{c\min}^{Df-3}] \quad 15$$

The water saturation is defined as the ratio of cumulative volume to the total pore volume, divide equation 13 by equation 15

$$S_w = \frac{v}{v_{\text{total}}} = \frac{\text{constant}}{Df-3} * \frac{[p_c^{Df-3} - p_{c\min}^{Df-3}]}{\left[ \frac{\text{constant}}{Df-3} * [p_{c\max}^{Df-3} - p_{c\min}^{Df-3}] \right]} \quad 16$$

But;  $p_{c\min} \ll p_c$ , then equation 16 will become

$$S_w = \left[ \frac{p_c}{p_{c\max}} \right]^{Df-3} \quad 17$$

Rearrange equation 7

$$p_c = \left[ \frac{[\sqrt{2} * \sigma * \cos\theta]}{[\sqrt{T_{cc}} * \sqrt{D_i}]} \right] \quad 18$$

Insert equation 18 into equation 17

$$S_w = \left( \frac{\left[ \frac{[\sqrt{2} * \sigma * \cos\theta]}{[\sqrt{T_{cc}} * \sqrt{D_i}]} \right]}{\left[ \frac{[\sqrt{2} * \sigma * \cos\theta]}{[\sqrt{T_{cc\max}} * \sqrt{D_i}]} \right]} \right)^{Df-3} \quad 19$$

Equation 19 after simplification will become

$$S_w = \left[ \frac{\sqrt{T_{cc\max}}}{\sqrt{T_{cc}}} \right]^{Df-3} = \left[ \frac{\sqrt{T_{cc}}}{\sqrt{T_{cc\max}}} \right]^{3-Df} = \left[ \frac{T_{cc}^{\frac{1}{2}}}{T_{cc\max}^{\frac{1}{2}}} \right]^{3-Df} \quad 20$$

Equation 20 is the prove of equation 1 which relate water saturation to cole cole time; maximum cole cole time and fractal dimension.

The capillary pressure can be scaled as

$$\log S_w = (D_f - 3) * \log P_c + \text{constant} \quad 21$$

Where  $S_w$  the water saturation,  $P_c$  the capillary pressure and  $D_f$  the fractal dimension

## Result and discussion

Based on field observation the Shajara Reservoirs of the Permo-Carboniferous Shajara Formation were divided here into three units as designated in Figure 1. These units from bottom to top are: Lower Shajara Reservoir, Middle Shajara reservoir, and Upper Shajara Reservoir. Their developed results of the Cole cole time fractal dimension and capillary pressure fractal dimension are shown in Table 1. Based on the achieved results it was found that the Cole cole time fractal dimension is equal to the capillary pressure fractal dimension. The maximum value of the fractal dimension was found to be 2.7872 assigned to sample SJ13 from the Upper Shajara Reservoir as confirmed in Table 1. Whereas the minimum value 2.4379 of the fractal dimension was recounted from sample SJ3 from the Lower Shajara reservoir as displayed in Table 1. The cole cole time fractal dimension and capillary pressure fractal dimension were witnessed to increase with increasing permeability as proofed in Table 1 owing to the possibility of having interconnected channels.

The Lower Shajara reservoir was symbolized by six sandstone samples (Figure 1), four of which considered as SJ1, SJ2, SJ3 and SJ4 as confirmed in Table 1 were carefully chosen for capillary pressure measurement. Their positive slopes of the first procedure and negative slopes of the second procedure are delineated in (Figure 2, Figure 3, Figure 4, Figure 5 and Table 1). Their cole cole time fractal dimension and capillary pressure fractal dimension values are proofed in Table 1. As we proceed from sample SJ2 to SJ3 a pronounced reduction in permeability due to compaction was reported from 1955 md to 56 md which reflects decrease in cole cole time fractal dimension and capillary pressure fractal dimension from 2.7748 to 2.4379 as specified in Table 1. Again, an increase in grain size and permeability was recorded from sample SJ4 whose Cole cole time fractal dimension and capillary pressure fractal dimension was found to be 2.6843 as described in Table 1.

In contrast, the Middle Shajara reservoir which is separated from the Lower Shajara reservoir by an unconformity surface as shown in Figure 1. It was designated by four samples (Fig. 1), three of which named as SJ7, SJ8, and SJ9 as illustrated in Table 1 were picked for capillary pressure measurement. Their positive slopes of the first procedure and negative slopes of the second procedure are displayed in (Figure 6, Figure 7, Figure 8 and Table 1). Their Cole cole time fractal dimensions and capillary pressure fractal dimensions show similarities as defined in Table 1. Their fractal dimensions are higher than those of samples SJ3 and SJ4 from the Lower Shajara Reservoir due to an increase in their permeability as elucidated in Table 1.

On the other hand, the Upper Shajara reservoir is separated from the Middle Shajara reservoir by yellow green mudstone as revealed in Figure 1. It is defined by three samples so called SJ11, SJ12, and SJ13 as explained in Table 1. Their positive slopes of the first procedure and negative slopes of the second procedure are exhibited in (Figure 9, Figure10, Figure 11 and Table 1). Moreover, Cole cole time fractal dimension and capillary pressure fractal dimension are also higher than those of sample SJ3 and SJ4 from the Lower Shajara Reservoir due to an increase in their permeability as explained in Table 1.

Overall a plot of Cole cole time fractal dimension versus capillary pressure fractal dimension as shown in Figure 12 reveals three permeable zones of varying Petro physical properties. Such variation in fractal dimension can account for heterogeneity which is a key parameter in reservoir quality assessment. This heterogeneity was also confirmed by plotting positive slopes of the first procedure versus negative slopes of the second procedure as proofed in Figure 13.

### **Conclusion**

The sandstones of the Shajara Reservoirs of the Permo-Carboniferous Shajara Formation were divided here into three units based on Cole cole time fractal dimension. The units from bottom to top are: Lower Shajara Cole Cole Time Fractal dimension Unit, Middle Shajara Cole Cole Time Fractal Dimension Unit, and Upper Shajara Cole Cole Time Fractal Dimension Unit. These units were also proved by capillary pressure fractal dimension. The fractal dimension was found to increase with increasing grain size and permeability.

### **Acknowledgement**


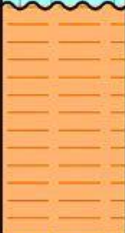
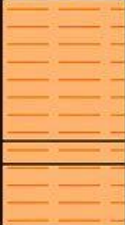
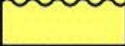
The author would like to thank King Saud University, College of Engineering, Department of Petroleum and Natural Gas Engineering, Department of Chemical Engineering, Research Centre at College of Engineering, and King Abdullah Institute for Research and Consulting Studies for their supports.

**References**

1. AlKhidir KEME. (2017). Pressure head fractal dimension for characterizing Shajara Reservoirs of the Shajara Formation of the Permo-Carboniferous Unayzah Group, Saudi Arabia. *Archives of Petroleum & Environmental Biotechnology*, 2017 (2): 1-7.
2. Al-Khidir KE. (2018). On Similarity of Pressure Head and Bubble Pressure Fractal Dimensions for Characterizing Permo-Carboniferous Shajara Formation, Saudi Arabia. *Journal of Industrial Pollution and Toxicity*, 1 (1): 1-10.
3. Alkhidir KEME. (2018) Arithmetic relaxation time of induced polarization fractal dimension for characterizing Shajara Reservoirs of the Shajara Formation. *Nanoscience and Nanotechnology*, 2 (1): 1-8.
4. Alkhidir KEME. (2018). Geometric relaxation time of induced polarization fractal dimension for characterizing Shajara Reservoirs of the Shajara formation of the Permo-Carboniferous Unayzah Group-Permo. *International Journal of Petrochemistry and Research*, 2 (1): 105-108.
5. AlKhidir KEME.(2018). Seismo Electric field fractal dimension for characterizing Shajara Reservoirs of the Permo-Carboniferous Shajara Formation. Saudi Arabia, *Petroleum & Petrochemical Engineering Journal*, 2 (4): 1-7.
6. Alkhidir KEME. (2018). Resistivity Fractal Dimension for Characterizing Shajara Reservoirs of the Permo Carboniferous Shajara Formation, Saudi Arabia. *International Journal of Petrochemical Science & Engineering*, 3 (3): 109-112.
7. Alkhidir KEME. (2018). Electro Kinetic Fractal Dimension for Characterizing Shajara Reservoirs of the Permo-Carboniferous Shajara Formation, Saudi Arabia. *International Journal of Nanotechnology in Medicine and Engineering*, 3 (4): 1-7.
8. Alkhidir KEME. (2019). Transverse Relaxation Time Fractal Dimension of Nuclear Magnetic Resonance for Characterizing Shajara Reservoirs of the Permo-Carboniferous Shajara Formation, Saudi Arabia. *Petroleum and Chemical Industry International*, 2 (2): 1-6.
9. Guo Y-h., Pan B-z., Zhang L-h., Fang C-h. (2018). Research and application of the relationship between transverse relaxation time and resistivity index in tight sandstone reservoir. *Journal of petroleum science and engineering*, 160:597-604.
10. Li K. & Horne R.N. (2002). Experimental verification of methods to calculate relative permeability using capillary pressure data. SPE 76757, Proceedings of the 2002 SPE Western Region Meeting/AAPG Pacific Section Joint Meeting held in Anchorage, Alaska. 2002.
11. Li K. & Willams W. (2007). Determination of capillary Pressure function from resistivity data, *Transport in Porous Media*, 67:1–15.

12. Toledo G T, Navy R A, Davis H T, & Scriven L E. (1994). Capillary pressure, water relative permeability, electrical conductivity and capillary dispersion coefficient of fractal porous media at low wetting phase saturation, SPE advanced technology Series. 2:136–141.
13. Wang Z, Pan M, Shi Y, Liu L, Xiong F, & Qin Z. (2018). Fractal analysis of Donghetang sandstones using NMR measurements. Energy & Fuels, 32 (3): 2973-2982.
14. Zhang Z & Weller A. (2014). Fractal Dimension of Pore-Space Geometry of Eocenesandstone Formation. Geophysics.79:D377-D387.



AGE	Fm.	Mbr.	unit	LITHO-LOGY	DESCRIPTION	
Late Permian	Khuff Formation	Huqayl Member			Limestone : Cream, dense, burrowed, thickness 6.56'	
Late Carboniferous - Permian	Shajara Formation	Upper Shajara Member	Upper Shajara mudstone		Sub-Khuff unconformity. Mudstone : Yellow, thickness 17.7'	
				Upper Shajar Reservoir	SJ13▲	Sandstone : Light brown, cross-bedded, coarse-grained, poorly sorted, porous, friable, thickness 6.5'
			SJ12▲		Sandstone : Yellow, medium-grained, very coarse-grained, poorly, moderately sorted, porous, friable, thickness 13.1'	
			SJ11▲			
			SJ10▲			
			Middle Shajara Member	Middle Shajara mudstone		Mudstone : Yellow-green, thickness 11.8' Mudstone : Yellow, thickness 1.3' Mudstone : Brown, thickness 4.5'
		Middle Shajara Reservoir			SJ10▲	Sandstone : Light brown, medium-grained, moderately sorted, porous, friable, thickness 3.6'
					SJ9▲	Sandstone : Yellow, medium-grained, moderately well sorted, porous, friable, thickness 0.9'
				SJ8▲		
		Lower Shajara Member		Lower Shajara Reservoir	SJ7▲	Sandstone : Red, coarse-grained, medium-grained, moderately well sorted, porous, friable, thickness 13.4'
					SJ6▲	Sandstone : White with yellow spots, fine-grained, hard, thickness 2.6'
			SJ5▲		Sandstone : Limonite, thickness 1.3'	
SJ4▲						
SJ3▲	Sandstone : White-pink, poorly sorted, thickness 1.6'					
SJ2▲	Sandstone : Yellow, medium-grained, well sorted, porous, friable, thickness 3.9'					
SJ1▲	Sandstone : Red, medium-grained, moderately well sorted, porous, friable, thickness 11.8'					
Early Devonian	Tawil Formation				Sub-Unayzah unconformity. Sandstone : White, fine-grained.	

SJ1 ▲ Samples Collection

Figure 1: surface type section of the Shajara Reservoirs of the Permo-Carboniferous Shajara Formation, latitude 26° 52' 17.4", longitude 43° 36' 18".

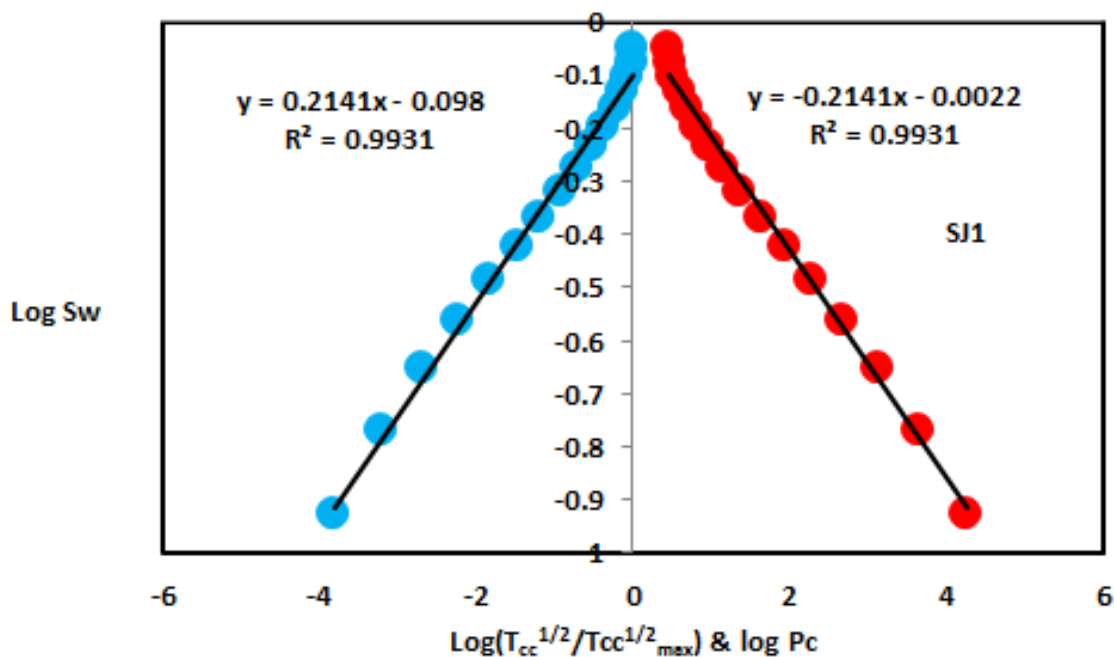


Figure 2:  $\text{Log}(T_{cc}^{1/2}/T_{ccmax}^{1/2})$  &  $\text{log Pc}$  versus  $\text{log Sw}$  for sample SJ1

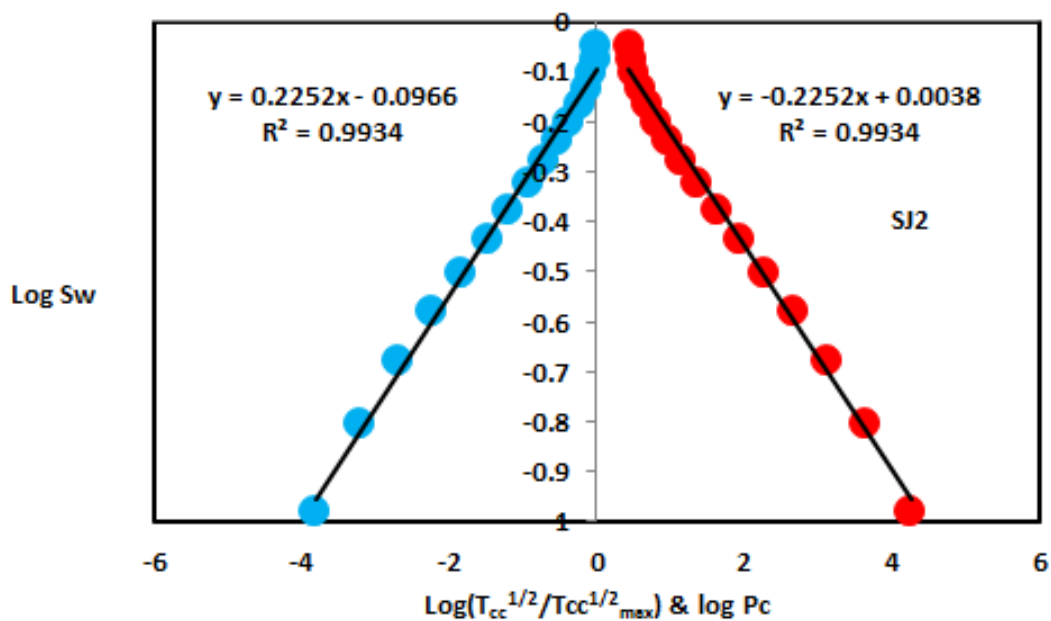


Figure 3:  $\text{Log}(T_{cc}^{1/2}/T_{ccmax}^{1/2})$  &  $\text{log Pc}$  versus  $\text{log Sw}$  for sample SJ2

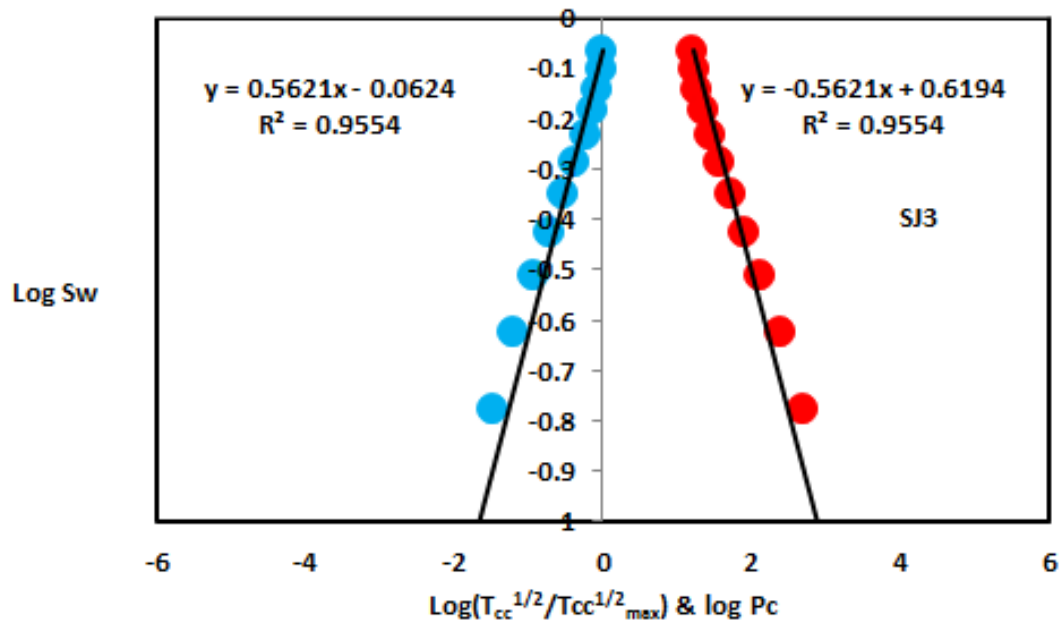


Figure 4:  $\text{Log}(T_{cc}^{1/2}/T_{ccmax}^{1/2})$  &  $\text{log Pc}$  versus  $\text{log Sw}$  for sample SJ3

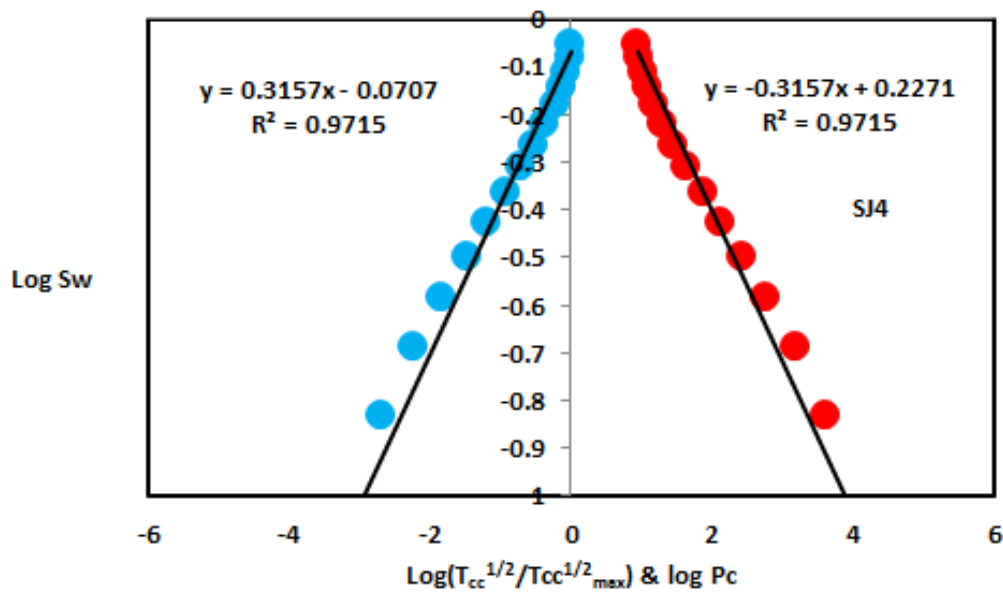


Figure 5:  $\text{Log}(T_{cc}^{1/2}/T_{ccmax}^{1/2})$  &  $\text{log Pc}$  versus  $\text{log Sw}$  for sample SJ4

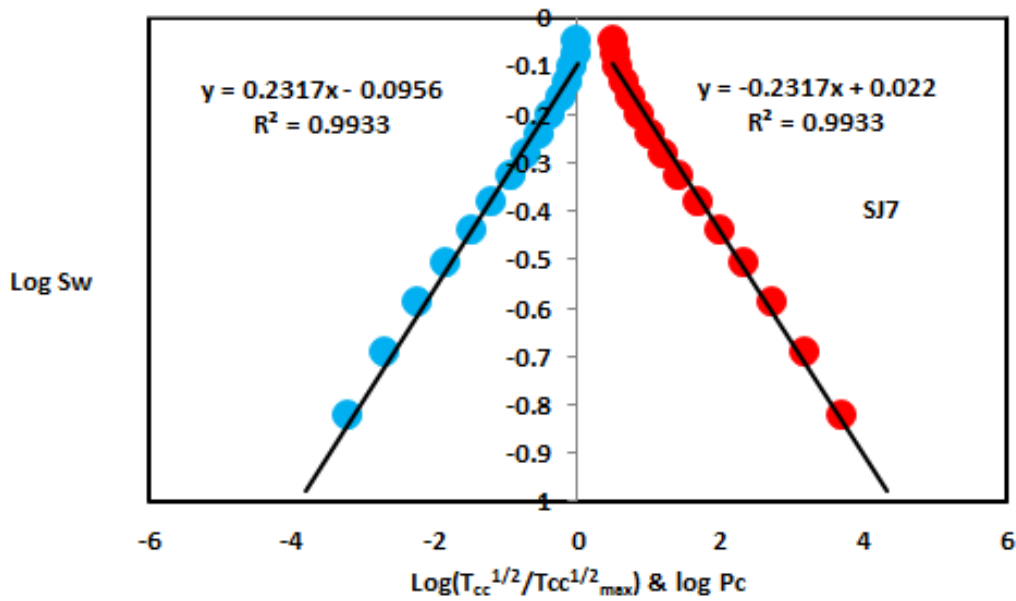


Figure 6:  $\text{Log}(T_{cc}^{1/2}/T_{ccmax}^{1/2})$  &  $\text{log Pc}$  versus  $\text{log Sw}$  for sample SJ7

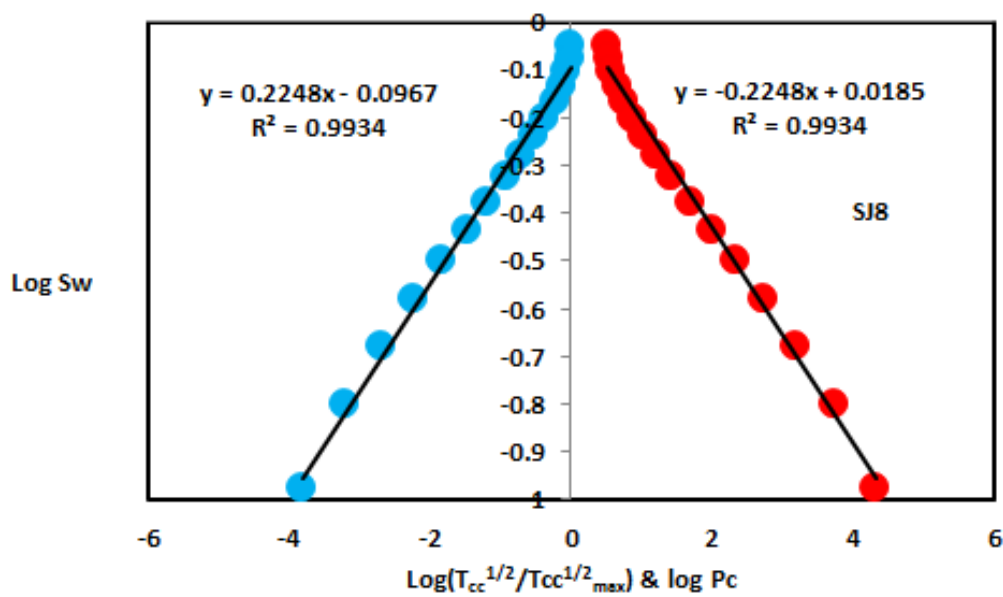


Figure 7:  $\text{Log}(T_{cc}^{1/2}/T_{ccmax}^{1/2})$  &  $\text{log Pc}$  versus  $\text{log Sw}$  for sample SJ8

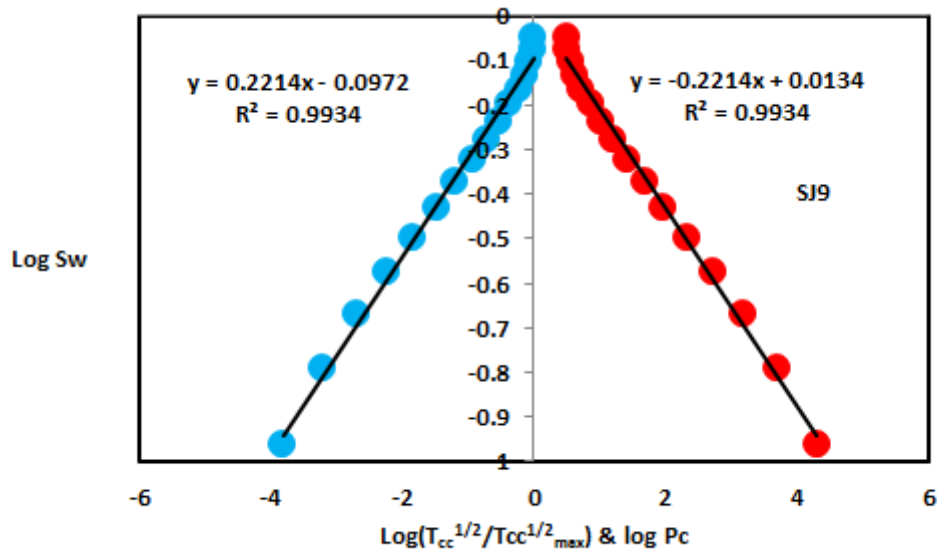


Figure 8:  $\text{Log}(T_{cc}^{1/2}/T_{ccmax}^{1/2})$  &  $\text{log Pc}$  versus  $\text{log Sw}$  for sample SJ9

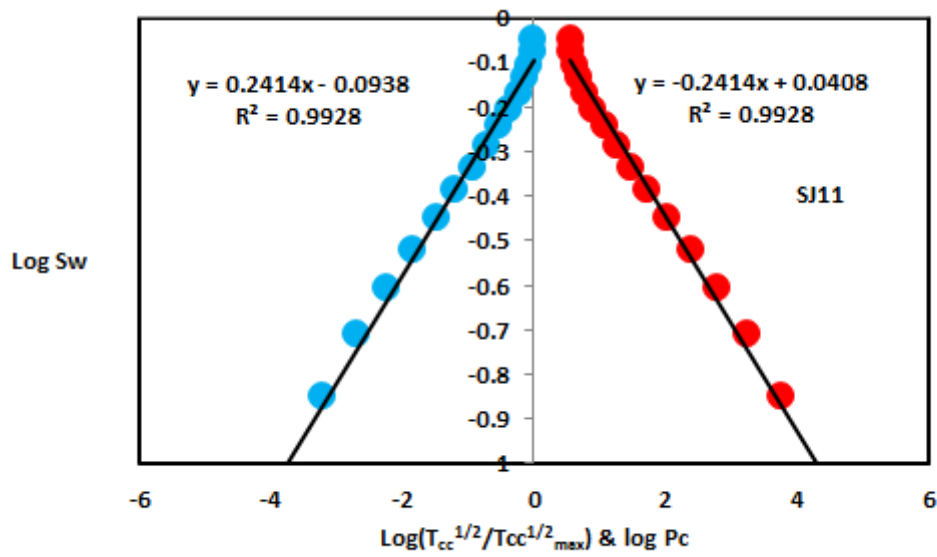


Figure 9:  $\text{Log}(T_{cc}^{1/2}/T_{ccmax}^{1/2})$  &  $\text{log Pc}$  versus  $\text{log Sw}$  for sample SJ11

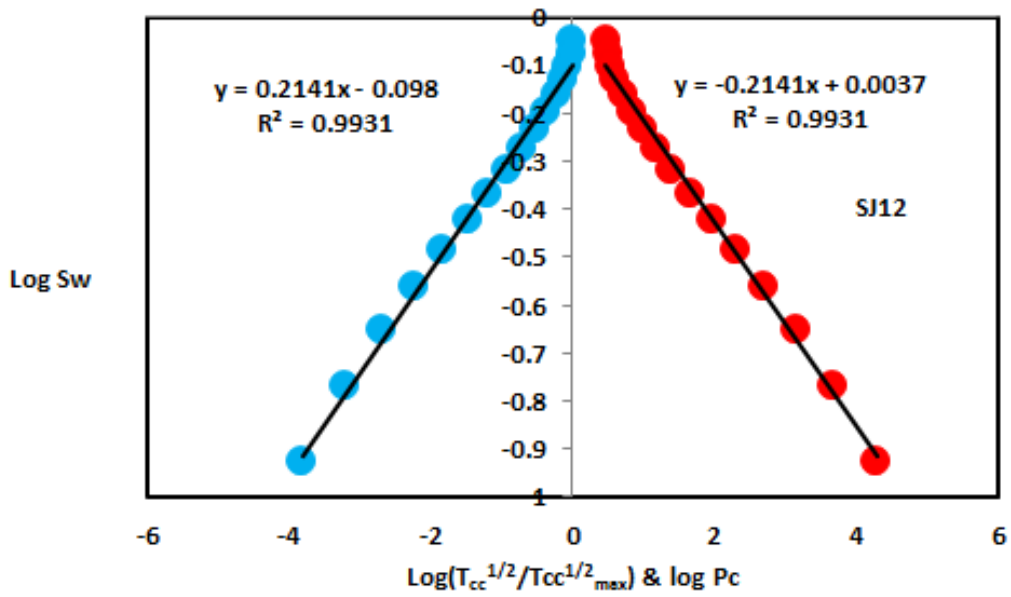


Figure 10:  $\text{Log}(T_{cc}^{1/2}/T_{CCmax}^{1/2})$  &  $\log Pc$  versus  $\log Sw$  for sample SJ12

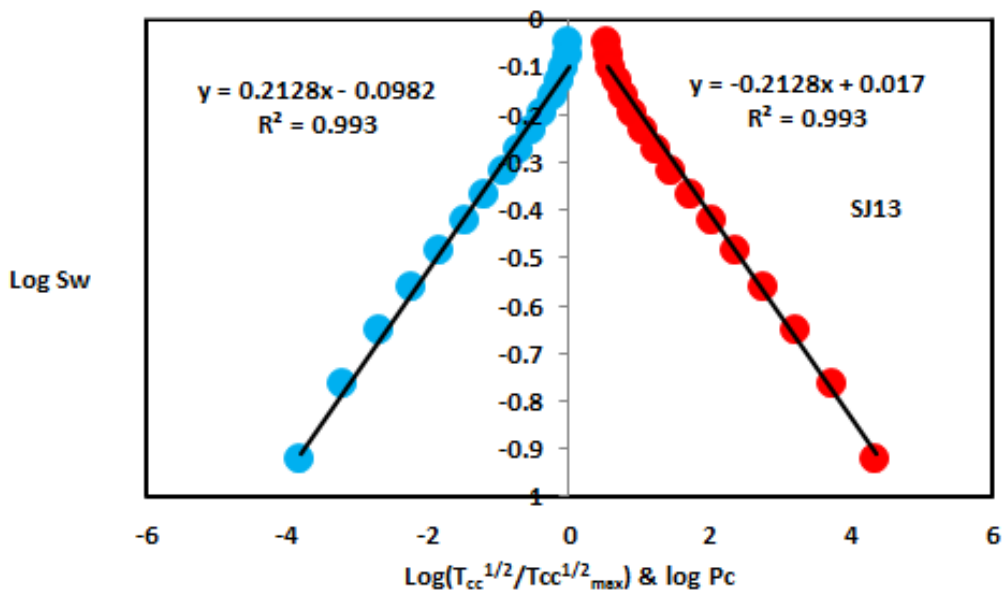


Figure 11:  $\text{Log}(T_{cc}^{1/2}/T_{CCmax}^{1/2})$  &  $\log Pc$  versus  $\log Sw$  for sample SJ13

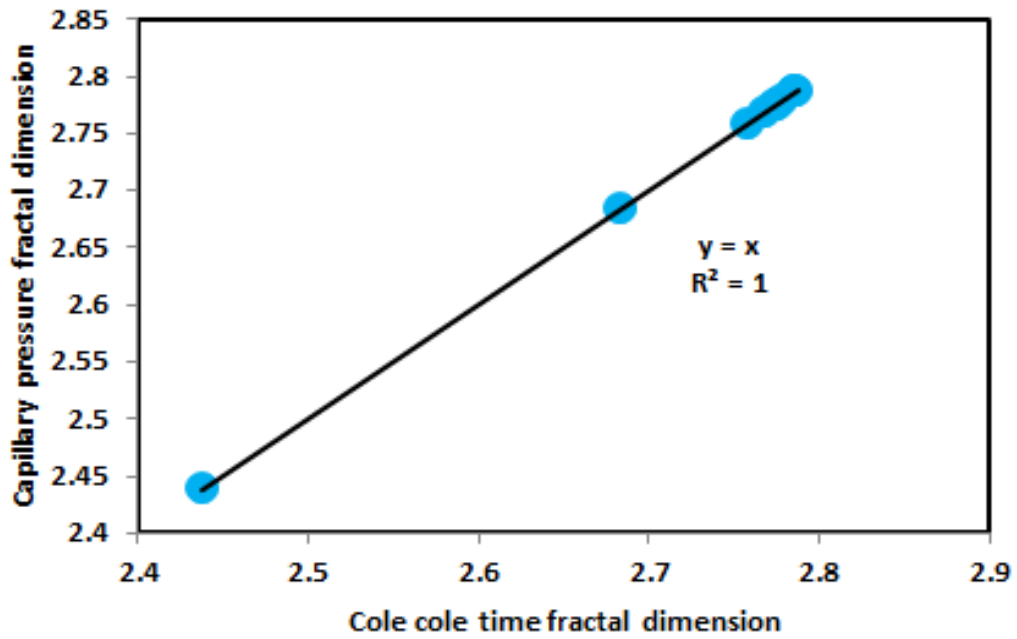


Figure 12: Cole cole fractal dimension versus capillary pressure fractal dimension

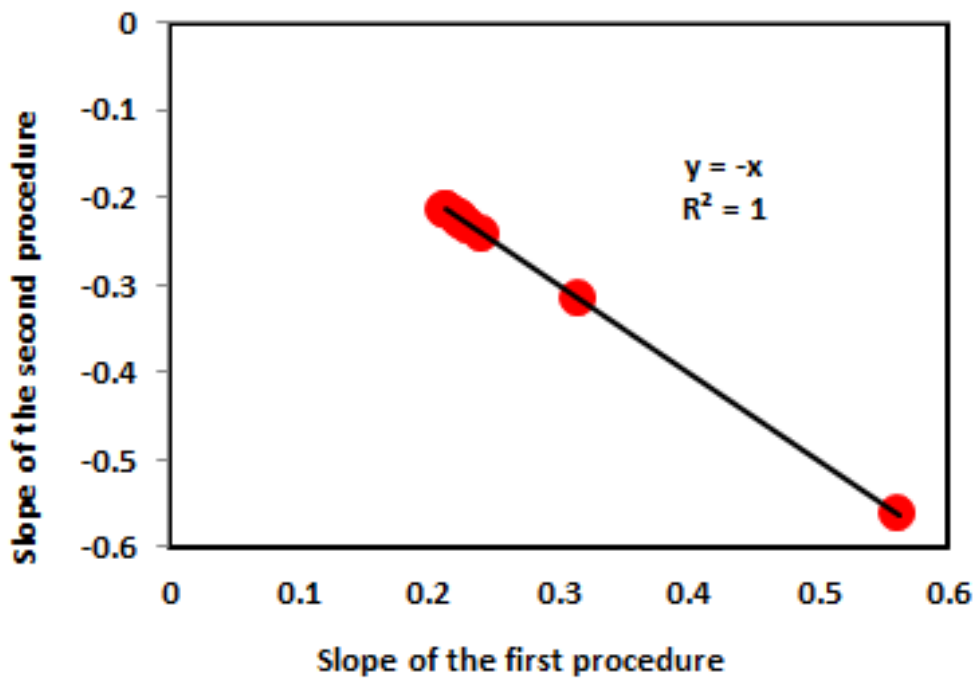


Figure 13: Slope of the first procedure versus slope of the second procedure

Table 1 Petro physical model showing the three Shajara Reservoir Units with their corresponding values of cole cole time fractal dimension and capillary pressure fractal dimension

Formation	Reservoir	Sample	Porosity %	k (md)	Positive slope of the first procedure Slope=3-Df	Negative slope of the second procedure Slope=Df-3	Cole cole fractal dimension	Capillary pressure fractal dimension
Permo-Carboniferous Shajara Formation	Upper Shajara Reservoir	SJ13	25	973	0.2128	-0.2128	2.7872	2.7872
		SJ12	28	1440	0.2141	-0.2141	2.7859	2.7859
		SJ11	36	1197	0.2414	-0.2414	2.7586	2.7586
	Middle Shajara Reservoir	SJ9	31	1394	0.2214	-0.2214	2.7786	2.7786
		SJ8	32	1344	0.2248	-0.2248	2.7752	2.7752
		SJ7	35	1472	0.2317	-0.2317	2.7683	2.7683
	Lower Shajara Reservoir	SJ4	30	176	0.3157	-0.3157	2.6843	2.6843
		SJ3	34	56	0.5621	-0.5621	2.4379	2.4379
		SJ2	35	1955	0.2252	-0.2252	2.7748	2.7748
		SJ1	29	1680	0.2141	-0.2141	2.7859	2.7859